Infectious Medicine 3 (2024) 100090

Contents lists available at ScienceDirect

Infectious Medicine

journal homepage: www.elsevier.com/locate/imj

Original Article

Rapid adaptive substitution of L226Q in HA protein increases the pathogenicity of H9N2 viruses in mice

Min Tan [a], Ye Zhang [a], Hong Bo [a], Xiyan Li [a], Shumei Zou [a], Lei Yang [a], Jia Liu [a], Qi Chen [a,b], Xiaohao Xu [a,b], Wenfei Zhu [a,*], Dayan Wang [a,*]

[a] National Institute for Viral Disease Control and Prevention, Chinese Center for Disease Control and Prevention, National Key Laboratory of Intelligent Tracking and Forecasting for Infectious Disease, Beijing 102206, China
[b] School of Public Health, Sun Yat-sen University, Guangdong 510275, China

ARTICLE INFO

Keywords:
Avian influenza virus
H9N2 subtype
Pathogenicity

ABSTRACT

Background: Since the first human infection with H9N2 virus was reported in 1998, the number of cases of H9N2 infection has exceeded one hundred by 2021. However, there is no systematic description of the biological characteristics of H9N2 viruses isolated from humans.

Methods: Therefore, this study analyzed the pathogenicity in mice of all available H9N2 viruses isolated from human cases in China from 2013 to 2021.

Results: Although most of the H9N2 viruses analyzed showed low or no pathogenicity in mice, the leucine to glutamine substitution at residue 226 (L226Q) in the hemagglutinin (HA) protein rapidly emerged during the adaptation of H9N2 viruses, and was responsible for severe infections and even fatalities. HA amino acid 226Q conferred a remarkable competitive advantage on H9N2 viruses in mice relative to viruses containing 226L, increasing their virulence, infectivity, and replication.

Conclusion: Thus, our study demonstrates that the adaptive substitution HA L226Q rapidly acquired by H9N2 viruses during the course of infection in mice contributed to their high pathogenicity.

1. Introduction

Avian influenza is an infectious disease that affects a variety of hosts, including birds, mammals, and humans [1]. Avian influenza virus (AIV) can be divided into 2 types based on differences in its pathogenicity in chickens: low pathogenic avian influenza virus (LPAIV) and highly pathogenic avian influenza virus [2]. Among all of the LPAIV subtypes, the H9N2 subtype is the most prevalent in poultry in China [2,3].

H9N2 AIV was first detected in turkeys in Wisconsin, USA, in 1966 [4]. It can be divided into North American and Eurasian lineages according to differences in the hemagglutinin (HA) gene. The Eurasian lineage mainly comprises BJ/94-like, Y439-like, Y280-like, and G1-like strains. H9N2 virus was isolated for the first time in China in 1994, in a chicken flock in Guangzhou, and then gradually adapted to poultry, ultimately becoming a dominant subtype in mainland China [2]. By the early 21st century [5], the H9N2 virus had generated a large number of genotypes through frequent genetic reassortment. During 1994 and 2013, Li et al. identified 117 H9N2 genotypes in China, with G57 genotype as the dominant genotype in 2013 [5,6]. The G57 genotype has provided the internal genes for several reassortant AIV subtypes, including H3N8, H7N9, and H10N8, which have been reported to infect humans [7–9].

H9N2 virus in poultry can directly infect humans. The first human case of H9N2 avian influenza was identified in 1998 [10], and cases of human H9N2 viral infection have been reported continuously since [11]. H9N2 AIV is endemic in China, where it has caused the highest number of human H9N2 infections worldwide. More than 100 cases of human H9N2 infection were reported by the end

* Corresponding authors.
E-mail addresses: zhuwf@ivdc.chinacdc.cn (W. Zhu), wangdayan@ivdc.chinacdc.cn (D. Wang).

https://doi.org/10.1016/j.imj.2024.100090
Received 21 November 2023; Received in revised form 4 December 2023; Accepted 10 December 2023

of 2021 globally [12]. However, a systematic description of the biological characteristics of H9N2 viruses isolated from humans is still lacking in the literature. To identify the features of H9N2 viruses from human cases and the changes over time, we investigated the pathogenicity of the H9N2 viruses isolated during 2013–2021 in China. The biological features and potential pathogenic mechanisms of these viruses were also comprehensively examined.

2. Methods

2.1. Ethics statement

All animal protocols were approved by the Ethics Committee of the National Institute for Viral Disease Control and Prevention, China Center for Disease Control and Prevention (CDC; 20210512037). All experiments involving live H9N2 viruses and animals were performed in biosafety level 2 (BSL2) facilities.

2.2. Cells and viruses

MDCK, DF1, and A549 cells were cultured in Dulbecco's modified Eagle's medium (DMEM; Gibco) containing 10% fetal bovine serum (Gibco), 1.5% HEPES (10 mM; Gibco), and 1% penicillin–streptomycin (100 units/mL; Gibco). Forty-three human H9N2 AIVs were isolated between 2013 and 2021, and were amplified in 9–10-day-old specific-pathogen-free (SPF) chicken embryos (Boehringer Ingelheim). After incubation at 37°C for 48 h, the allantoic fluid of the virus-infected embryonated eggs was collected and stored at −80°C until use. The virus was titrated in MDCK cells to determine the 50% tissue culture infectious dose ($TCID_{50}$) with the Reed–Münch method.

2.3. Virus sequencing

In this study, we used the Illumina next-generation sequencing (NGS) technology (Illumina Inc.) to sequence and analyze the H9N2 influenza viruses [13–15]. Viral RNA was extracted from the viruses with the MagMAX CORE Nucleic Acid Purification Kit (Thermo Fisher Scientific). The extracted RNA was reverse transcribed to cDNA, and PCR amplification was performed with the SuperScript III One-Step RT-PCR System (Thermo Fisher Scientific) with primers targeting the influenza virus genome. The resulting amplicons were purified and subjected to NGS on the MiSeq platform (Illumina). The raw sequencing data were preprocessed to remove low-quality reads, adapter sequences, and contaminants. The remaining high-quality reads were assembled de novo with multiple software tools, including Velvet (version 1.2.10) and Newbler (version 2.5). All AIV contigs obtained were subjected to quality control and analyzed for sequence similarity and genetic variation against the GISAID (http://www.gisaid.org). The influenza virus sequences with greatest similarity were selected as references against which the reads were mapped with Bowtie 2 (version 2.1.0). The *influenza A virus* genome sequences were obtained by extracting consensus sequences from the mapping results. Each site on the 8 genomic segments had a coverage depth of at least 30 ×.

2.4. Recombinant plasmid construction and virus rescue

Synthesized gene fragments of H9N2 viruses from human cases were recombined with the bidirectional pHW2000 vector to form recombinant plasmids. The leucine to glutamine substitution at residue 226 (L226Q) was introduced into the HA gene in each strain with the Q5 Site-Directed Mutagenesis Kit (New England Biolabs), according to the manufacturer's instructions. MDCK and 293T cells were transfected with 8 recombinant reverse-genetic plasmids of influenza virus. After 24 h, 9-day-old SPF chicken embryos or MDCK cells were inoculated with the cell supernatants containing the recombinant viruses and incubated at 37°C for 48 h. All reassortant viruses were verified with Illumina NGS.

2.5. Growth properties in vitro

To test viral replication *in vitro*, monolayers of MDCK, DF1, and A549 cells were washed 3 times with phosphate-buffered saline (PBS) and inoculated with viruses at a multiplicity of infection (MOI) of 0.001. After viral adsorption for 1 h, the viral inoculum was removed and DMEM containing 2 mg/mL TPCK trypsin (Sigma-Aldrich) was added to the cell culture dishes. The cell supernatants were collected after 0, 6, 12, 24, 36, 48, 60, and 72 h. The viral titers in the supernatants were determined in MDCK cells.

2.6. In vivo experiments in mice

Eight-week-old SPF female C57BL/6J mice, from Beijing Vital River Laboratory Animal Technology Co., Ltd, were used to assess the pathogenicity of the H9N2 AIVs. In all experiments, the mice were infected with specific titers (in a volume of 50 μL) of H9N2 virus (n = 5 per group) in nasal drops after respiratory sedation (with isoflurane). Drops (50 μL) of PBS were used as the controls. The bodyweight and survival of the mice were monitored daily for 14 days. Mice that lost 25% of their bodyweight were humanely euthanized.

Serum samples from the surviving mice were collected at 14 days postinfection (dpi), treated with receptor-disrupting enzyme (Denka Seiken) for 16–18 h at 37°C, and inactivated at 56°C for 30 min. The treated serum samples were tested for their HA-inhibiting (HI) antibody

titers with 0.5% (vol/vol) turkey erythrocytes. HI titers >10 were considered antibody-positive [16]. The Karber method was used to calculate the 50% median lethal dose (MLD_{50}) [17,18].

We tested the viral loads of the nasal clip, trachea, and lung at 1, 3, and 5 dpi, and those of the kidney, heart, brain, liver, and small intestine at 5 dpi ($n = 3$ per group). The organs were collected and homogenized in 1 mL of PBS containing antibiotics, and the viral titers of these tissues were determined using MDCK cells [19].

2.7. Histopathology and immunohistochemistry

At 1, 3, and 5 dpi, the right upper lung lobes of the mice ($n = 3$ per group) were fixed in 10% formalin, embedded in paraffin, and cut into 3–5 mm thick sections. The sections were stained with hematoxylin and eosin (HE) and observed under a light microscope.

The mouse lung tissue sections were immunohistochemically stained. The pretreated dewaxed tissues were treated with 0.1 M citrate buffer (pH 6.0) for antigen retrieval. The processed tissue sections were immunostained for viral nucleoprotein (NP) with a primary monoclonal anti-*influenza A virus* NP antibody (ab20841, Abcam, Cambridge, UK) with incubation overnight at 4°C. The tissue sections were then incubated with a horseradish peroxidase (HRP)-conjugated rabbit antigoat IgG (H&L) secondary antibody (ZB-2306, ZSGB-BIO, Beijing, China) for 60 min at room temperature, while protected from the light. Finally, the nuclei were stained with 4′,6-diamidino-2-phenylindole (DAPI) and the tissue sections were sealed and observed under microscopy.

2.8. Quantitative real-time PCR to determine cytokine and chemokine expression

To investigate the differences in the mRNA expression of immune factors in mice after viral infection, we extracted the total RNA from mouse lung tissue homogenates with a Nucleic Acid Extraction System (IANLONG), according to the manufacturer's instructions. The RNA was reverse transcribed to cDNA with a Prime Script RT reagent Kit with gDNA Eraser (Takara, Cat no. RR047A). The $2^{-\Delta\Delta t}$ method was used to calculate the expression of each gene relative to that of *Gapdh*. Each experiment included 3 technical replicates for each sample and 3 experimental replicates.

2.9. Direct receptor-binding analysis

The receptor preference of each virus was determined with a solid-phase direct binding assay, as described previously [20], with minor modifications. We used 2 different synthetic sialylglycopolymers containing either α2,3-linked sialic acid (Neu5Aca2-3Galb1-4GlcNAcb-SpNH-PAA, 3′-SLN) or α2,6-linked sialic acid (Neu5Aca2-6Galb1-4GlcNAcb-SpNH-PAA, 6′-SLN) (Glyco Tech Corporation). The 2 synthetic sialyglycopolymers (3′-SLN and 6′-SLN) were diluted 2-fold with PBS and added to clear microtiter plates (Costar 3590). The microplates were incubated overnight at 4°C and then exposed to ultraviolet light (254 nm) for 10 min. After the glycopolymer solution was removed, the plates were washed 3 times with ice-cold PBST (PBS containing 0.1% Tween 20), inoculated with 64 HA units of H9N2 virus, and incubated overnight at 4°C. The plates were washed 5 times with PBST and then incubated for 1 h at 37°C with a monoclonal antibody directed against the HA of the Flu/A/NP antibody (Zoonogen). The plates were washed 5 times with PBST, and incubated for 1 h at 37°C with an HRP-conjugated goat antihuman IgG antibody (ZSGB-BIO). After 5 more washes, the plates were incubated with tetramethylbenzidine (Sigma Aldrich), the activity of which was stopped with 0.2 M H_2SO_4. The optical density of each sample at 450 nm was measured in duplicate with an Epoch Microplate Spectrophotometer (BioTek). The H5N1 virus (RG-A/Anhui/1/2005) was used as the binding control.

2.10. Statistical analyses

All statistical analyses were performed with the GraphPad Prism version 9.0 software (GraphPad software Inc.). Statistical significance was determined with the Student's *t* test and $p < 0.05$ was considered statistically significant.

3. Results

3.1. Divergent pathogenicity profiles of H9N2 viruses in mice

We inoculated mice with 43 H9N2 viruses isolated from infected humans to investigate viral pathogenicity (Table S1, S2). After infection with 10^7 $TCID_{50}$ of the H9N2 viruses, the bodyweights of most mice did not change significantly over the following 14 days (Fig. S1), with the exception of mice infected with strain A/Hubei-songzi/1631/2019 (HB-1631), A/Hunan/11173/2020 (HN-11173), or A/Guangdong/00470/2021 (GD-00470), which showed significant bodyweight losses. For GD-00470, 3 of 5 mice lost more than 25% of their bodyweight at 8 or 9 dpi, whereas the other 2 mice showed a weight loss of <25% and gradually recovered (Fig. S1). HN-11173 caused bodyweight losses of <20% in 4 mice and a loss of >25% in 1 mouse at 5–10 dpi (Fig. S1). The mice infected with HB-1631 displayed significant weight loss at 4 dpi, and all died at 6 dpi (Fig. S1).

3.2. L226Q substitution in HA protein

Sequence analysis was performed to investigate the mechanism underlying the higher pathogenicity of HB-

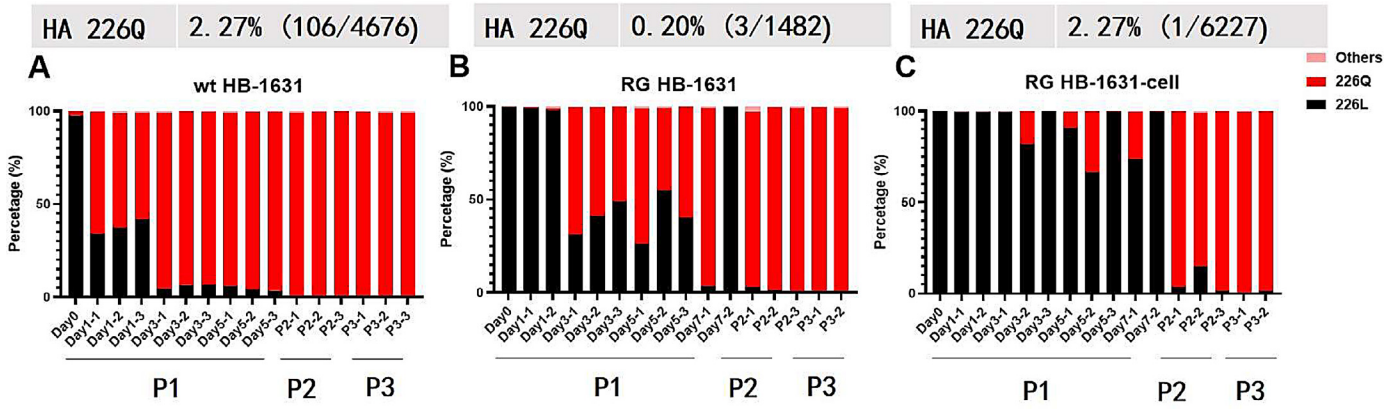

Fig. 1. Mutational trends at HA residue 226 in wild virus and rescued viruses. Twelve mice were infected with 105 TCID50 of wild-type (wt) HB-1631 (A), RG HB-1631 (B), and RG HB-1631-cell virus (C). Lung tissues from 3 mice per group were collected on 1, 3, 5, and 7 dpi for subsequent sequencing analysis. Lung homogenates from the 3 mice sampled on day 3 were used to infect another batch of mice to investigate viral propagation *in vivo*.

1631, HN-11173, and GD-00470. A critical pathogenic molecular marker, the E/K627K substitution in the polymerase basic 2 (PB2) gene, was identified in the lung tissues of mice infected with GD-00470. However, no adaptive mutations were observed in the lung tissues of mice infected with HN-11173. After comparing the sequences of wild-type (wt) HB-1631 virus and virus sequences from the lung tissue of mice infected with wt HB-1631, we identified the substitution L226Q (H3 numbering) in the HA protein sequences. Deep sequencing showed that the proportion of reads containing Q at residue 226 of HA increased during the HB-1631 infection process in mice (Fig. 1A), occurring in 61% ± 4%, 94% ± 1%, and 95% ± 1% of reads at 1, 3, and 5 dpi, respectively (Table S3). Whereas for the original wt strain HB-1631(wt HB-1631), 2.27% (106/4676) of reads contained the L226Q substitution.

3.3. Rapid selection for HA L226Q during H9N2 infection in mice

To investigate the adaptation process of H9N2 viruses in mice at residue 226 of the HA protein, we constructed the reassortant virus RG HB-1631 containing 226L. After mice were infected with different concentrations of either RG HB-1631 (RG HB-1631 amplified with chicken embryos) or RG HB-1631-cell (RG HB-163 amplified with MDCK cells), their lung tissues were collected on 1, 3, 5, and 7 dpi. The viruses isolated from lung tissues on 3 dpi were used to inoculate the mice of the next passage. The lung homogenate samples collected from this second batch of infected mice on day 3 were designated P2-1, P2-2, and P2-3. Viral passage was continued, and the lung homogenate samples from 3 mice on day 3 after the third round of infection were designated P3-1, P3-2, and P3-3. Few reads containing the HA 226Q substitution were detected from either the RG HB-1631 or RG HB-1631-cell virus in passage 1 (P1), accounting for 0.20% (3/1482) and 0.02% (1/6227) of the total reads, respectively. After inoculation in P2, the HA L226Q substitution had clearly increased at 3 dpi in most mice infected with RG HB-1631 (Fig. 1B), whereas although the HA L226Q substitution also increased in some RG HB-1631-cell-infected mice, the increase was less marked than in RG HB-1631 (Fig. 1C). However, the proportion of HA 226Q exceeded 84% in the P2 generation of both RG HB-1631 and RG HB-1631-cell virus, and was nearly 100% in the P3 generation.

To investigate the selection of HA L226Q in other H9N2 strains, 3 viruses (A/Hunan/11173/2020, A/Hunan/34179/2018, and A/Guangdong/12902/2021) containing HA 226L were selected for passage in mice. The sequencing results showed that the proportion of HA 226Q reads exceeded 98% in the lung tissues of all of the infected mice in both the P3 and P4 generations (Table S3). This result indicated that the HA L226Q mutation rapidly occurred during viral replication in the lungs of mice, and was commonly observed in these human H9N2 isolates.

3.4. HA L226Q alters the pathogenicity of H9N2 viruses in mice

We rescued the RG HB-1631-226Q virus carrying the HA L226Q mutation. After mice were inoculated with 10^7 $TCID_{50}$ RG HB-1631-226Q, their bodyweights started to decrease at 2 dpi, and all of the mice died at 4 dpi (Fig. 2A). The mice infected with the reassortant virus showed a faster bodyweight loss than the wt HB-1631-infected mice (Fig. S2). To confirm this, we rescued another strain of H9N2 virus, RG HN-34179, and obtained RG HN-34179-226Q carrying HA 226Q. The HA L226Q mutation also increased the pathogenicity of RG HN-34179 in mice (Fig. 2A).

To investigate the dose dependence of pathogenicity conferred by HA L226Q, 5 mice in each group were in-

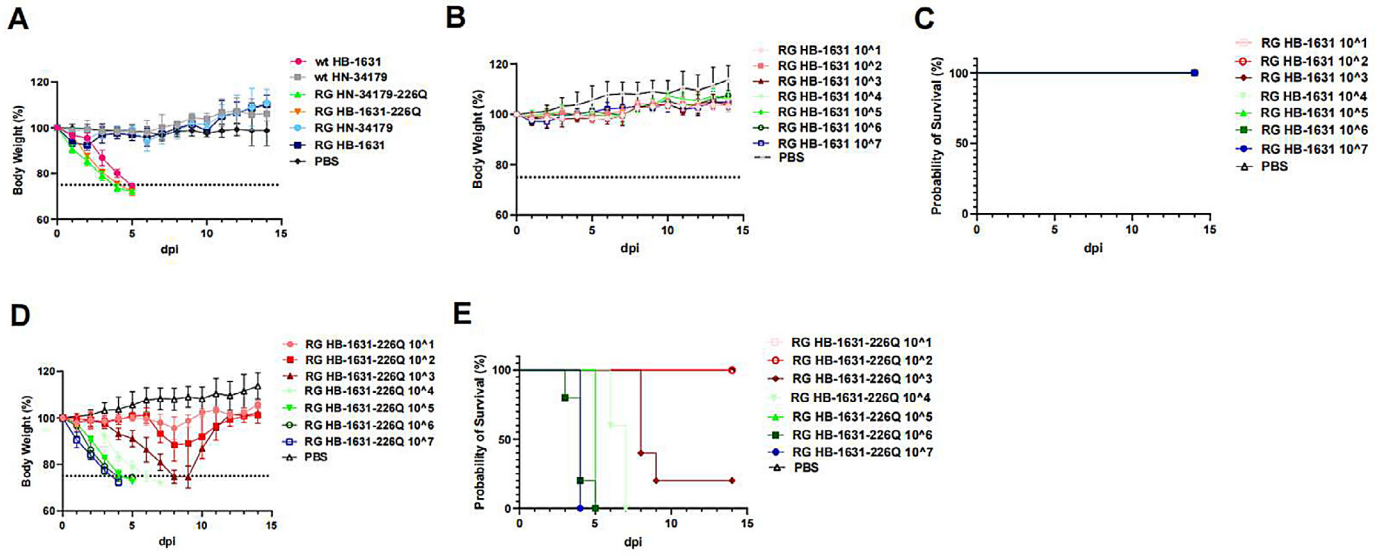

Fig. 2. HA L226Q increased the virulence of H9N2 viruses in mice. Five C57/6J mice per group were inoculated with the indicated viruses or mock infected with PBS. (A) Bodyweight changes of the mice infected with wt HB-1631, RG HB-1631, or RG HB-1631-226Q (107 TCID50) for 14 dpi. Bodyweight changes in mice infected with 101–107 TCID50 of RG HB-1631 (B) or RG HB-1631-226Q (D) at 14 dpi. Values represent the average bodyweights ± standard deviations of 5 mice compared with the baseline weight. Survival of mice infected with RG HB-1631 (C) or RG HB-1631-226Q (E). Mice that lost more than 25% of their initial bodyweight were considered at the experimental endpoint and were humanely euthanized.

fected with 10^1–10^7 $TCID_{50}$ RG HB-1631-226Q or RG HB-1631. All RG HB-1631-infected mice survived and showed no significant reduction in bodyweight (Fig. 2B, C). By contrast, the mice inoculated with RG HB-1631-226Q showed bodyweight loss at the low dose of 10^2 $TCID_{50}$ (Fig. 2D). All mice infected with RG HB-1631-226Q at 10^4-10^7 $TCID_{50}$ (Fig. 2D, E) showed clinical signs of disease, such as depression, loss of appetite, severe wasting, lusterless hair, arching of the back, and ultimately death. In summary, the MLD_{50} of RG HB-1631-226Q was $10^{2.7}$ $TCID_{50}$, whereas the 50% median lethal dose (MLD_{50}) of RG HB-1631 was > $10^{7.5}$ $TCID_{50}$.

After 14 days of viral infection, the HI titers in the sera of the surviving mice were measured. The 50% median infectious dose (MID_{50}) of RG HB-1631-226Q was $<10^{0.5}$ $TCID_{50}$, whereas the MID_{50} of RG HB-1631 was $10^{3.3}$ $TCID_{50}$ (Table 1).

3.5. HA L226Q induced pathological changes and proinflammatory responses to H9N2 viruses in mice

Although most mice infected with RG HB-1631 showed no weight loss, HE staining showed that both RG HB-1631-226Q and RG HB-1631 infection caused progressive lesions after inoculation with 10^7 $TCID_{50}$ (Fig. 3A) or 10^5 $TCID_{50}$ (Fig. S3A). Small amounts of exudate and foam cells were observed in the trachea, bronchi, and thickened mucosal epithelia of each group of 3 mice (Figs 3A, S3A). However, the interstitial lung tissues of the mice infected with RG HB-1631-226Q displayed more vascular congestion and more pronounced inflammatory cell infiltration, including neutrophils and macrophages; alveolar fusion was detected in about one-third of the lung, and emphysema was more pronounced than in the RG HB-1631-infected mice.

Immunohistochemical staining showed more virus-positive cells in both the bronchial epithelial and alveolar tissues of the RG HB-1631-226Q-infected lungs than the RG HB-1631-infected lungs (Figs 3B, S3B). Whereas RG HB-1631 was mainly distributed around the bronchial epithelial cells, RG HB-1631-226Q had a wider distribution around both the bronchial epithelial cells and alveolar cells. Moreover, the RG HB-1631-226Q virus induced higher levels of tumor necrosis factor α (TNF-α), macrophage inflammatory protein 1α (MIP-1α), toll-like receptor 2 (TLR2), cluster of differentiation 14 (CD14), CD3, and interleukin 1β (IL1β) (Fig. S4). These results indicate that HA L226Q induces elevated pathological changes and proinflammatory responses to H9N2 viruses in mice.

3.6. HA L226Q increases the replication of H9N2 viruses

We infected MDCK, DF1, and A549 cells (MOI = 0.01) with RG HB-1631 or RG HB-1631-226Q. Similar viral replication profiles were observed in MDCK and A549 cells (Fig. S5A–C); however, in DF1 cells, RG HB-1631-226Q produced more progeny virus at 24 and 36 h post-infection (hpi) than in the other 2 cell types (Fig. S5B).

We further measured the viral titers in the mouse nasal turbinate, tracheal, and lung tissues at 1, 3, and 5 dpi, and showed that RG HB-1631-226Q produced significantly higher titers than RG HB-1631 at 1 and 5 dpi ($p < 0.05$) (Fig. 3C). These findings suggest that HA-226Q viruses

Table 1
Hemagglutinin inhibition antibody test of the C57BL/6J mice inoculated with RG HB-1631 and RG HB-1631-226Q viruses.

viruses	Inoculation dose (log10 $TCID_{50}$)	HI titers[a]					MID_{50} ($logTCID_{50}$)[b]
		#1	#2	#3	#4	#5	
RG HB-1631	7	1280	1280	1280	1280	1280	3.3
	6	1280	1280	1280	1280	1280	
	5	640	1280	1280	1280	1280	
	4	1280	640	640	320	320	
	3	320	20	<10	20	20	
	2	<10	<10	<10	<10	<10	
	1	<10	<10	<10	<10	<10	
RG HB-1631-226Q	7	ND	ND	ND	ND	ND	0.5
	6	ND	ND	ND	ND	ND	
	5	ND	ND	ND	ND	ND	
	4	ND	ND	ND	ND	ND	
	3	640	ND	ND	ND	ND	
	2	320	320	320	640	640	
	1	320	320	320	320	80	
PBS		<10	<10	<10	<10	<10	

[a] Serum was collected from each survival mouse at 14dpi, and tested for hemagglutination inhibition titers against the respective virus.
[b] 50% mouse infection dose, and was determined using the Karber Method.ND, not determined due to death of mice (treated as positive).These data demonstrate that the virulence of the RG HB-1631-226Q virus was greater than that of the RG HB-1631 virus in mice.

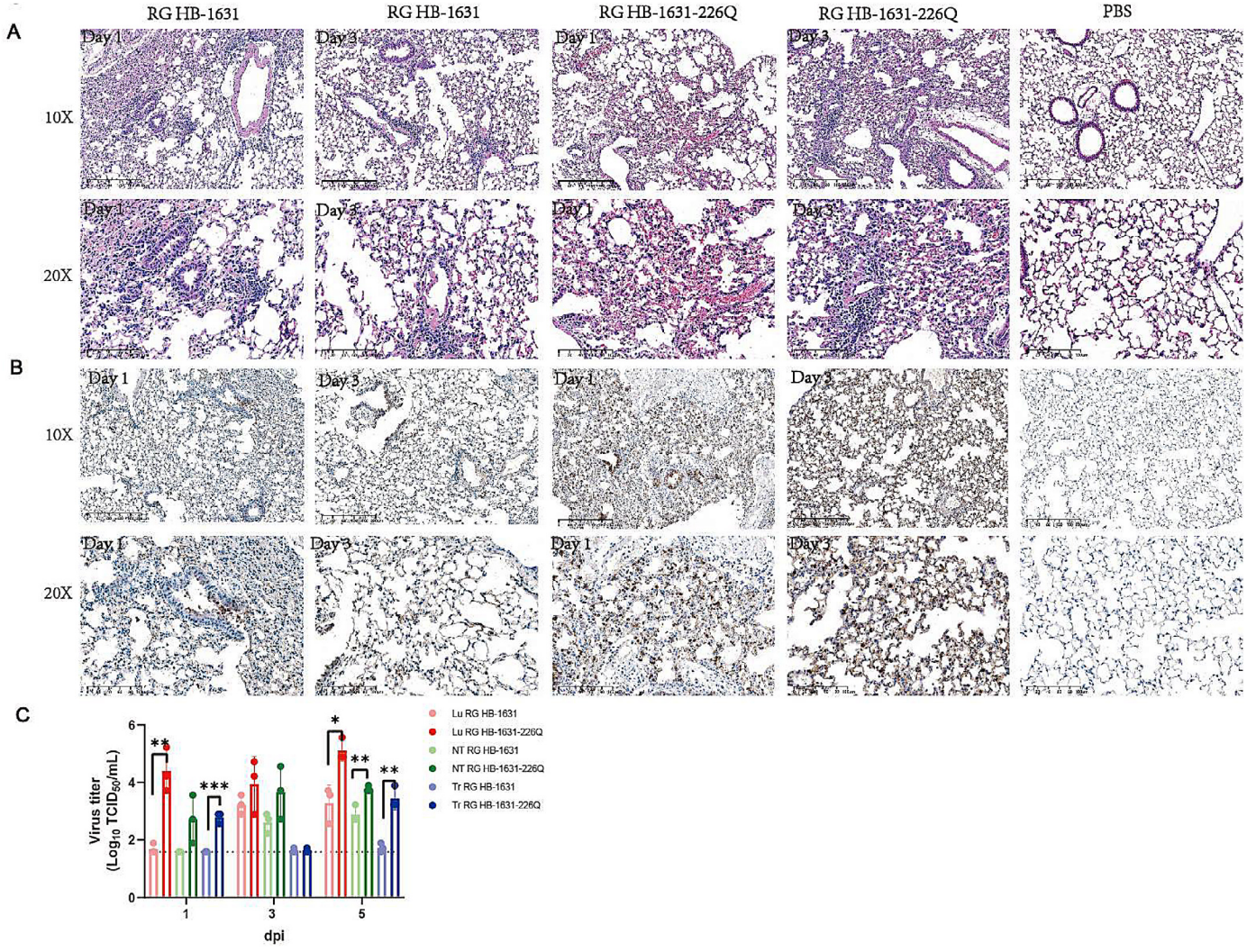

Fig. 3. HA L226Q increased the pathogenicity of H9N2 viruses in mice. Mice were infected with 107 TCID50 of RG HB-1631 virus or RG HB-1631-226Q mutant. The right upper lobe of each lung was collected at 1- and 3-days postinfection (dpi, i.e., at 1 timepoint), fixed in 10% formalin, embedded in paraffin, and sectioned. Sections were stained with hematoxylin and eosin (HE, A) or immunohistochemically stained (IHC, B). Nose clips (NT), tracheae (Tr), and lungs (Lu) were collected on 1, 3, and 5 dpi, and viral titers were determined with endpoint titration in MDCK cells. (C) Each patterned bar represents the average viral titer calculated for 3 mice. The black-dashed horizontal line indicates the lower limit of detection. $^{*}p < 0.05$, $^{**}p < 0.01$, $^{***}p < 0.001$.

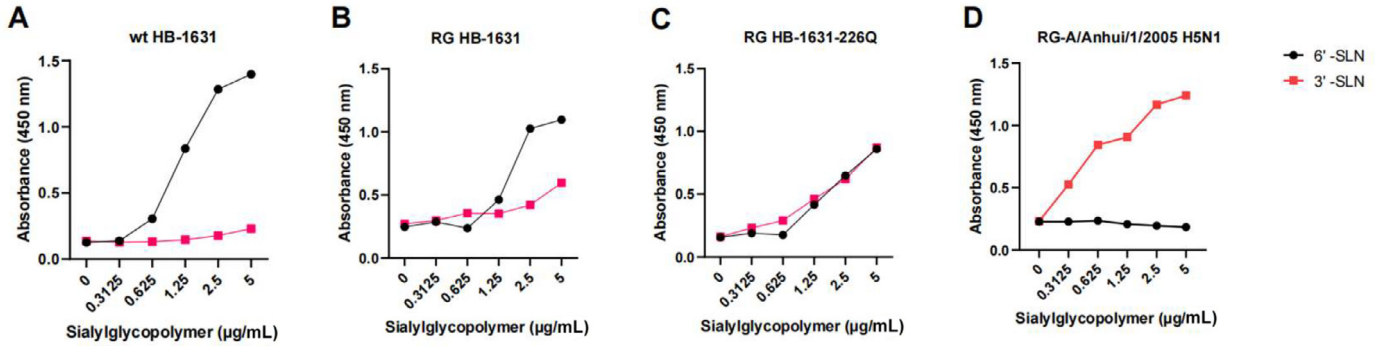

Fig. 4. HA L226Q alters H9N2 receptor-binding affinity. Receptor-binding affinities of wild-type (wt) HB-1631 (A), RG HB-1631 (B), RG HB-1631-226Q (C), and RG-A/Anhui/1/2005 H5N1 (D). The binding affinities of the viruses to 2 different biotinylated glycans (6′-sialyl-N-acetyllactosamine [6′-SLN] shown in dark; 3′-sialyl-N-acetyllactosamine, [3′-SLN] shown in red) were determined, and the viruses were analyzed at concentrations of 0.3125, 0.625, 1.25, 2.5, and 5 μg/mL. Every experiment was conducted twice, and the absorbance was read at 450 nm. The avian H5N1 influenza virus (RG-A/Anhui/1/2005) was used as an early-stage virus control. The receptor-binding affinity of the virus is expressed as the mean ± SD.

replicate more efficiently than HA-226L viruses in the lungs of mice.

3.7. HA H226Q alters the viral receptor-binding properties

A solid-phase direct binding assay showed that in contrast to A/Anhui/1/2005 (H5N1), which preferentially bound to the α2,3-SA receptor, wt HB-1631 and RG HB-1631 preferentially bound to the α2,6-SA receptor (Fig. 4A, B), whereas RG HB-1631-226Q showed no preference and bound to both receptors (Fig. 4C), suggesting that the HA L226Q mutation alters the specificity of H9N2 viruses.

4. Discussion

The key findings of the present study are as follows. Forty-three strains of human-infecting H9N2 viruses were screened by inoculation in mice and 3 strains possessed higher pathogenicity. Sequence analysis showed that the rapid amino acid substitution L226Q in HA mediated the increased pathogenicity of H9N2. HA L226Q also increased the virulence and replication of H9N2 and the inflammatory damage in mice. Although strains such as HN-34179 developed L226Q after multiple mouse lung tissue passages, the original strain with HA 226L had low pathogenicity in mice after initial infection with high viral titers, indicating the significance of this specific mutation in determining pathogenicity.

Avian influenza has undergone adaptive amino acid mutations during its adaptation to mammals, leading to pathological changes in the virus [21]. For example, mutations at E627K [22] and D701N [23] in PB2 of the H9N2 viruses increase their virulence and replication capacities. Combined mutations in HA (L226Q) and PB2 (M147L, V250G, or E627K) or HA (L226Q) and M1 (R210K) significantly increase the virulence of the H9N2 chicken isolate in mice, whereas the single mutation HA L226Q only increases viral replication [24]. In the present study, we confirmed the substitution of L226Q in H9N2 viruses from human cases caused phenotypic changes and increased the pathogenicity of the virus in mice. Our animal experiments also showed that viruses with HA 226Q had a competitive advantage in mice over viruses with HA 226L. The proportion of HA 226Q exceeded 84% in the P2 generation and was nearly 100% in the P3 generation of mice inoculated with RG HB-1631 virus.

Notably, the L226Q substitution in HA destroyed the binding preference of the virus for the α2,6-SA receptor, allowing it dual-receptor binding ability, binding to both α2,3-SA and α2,6-SA receptors.

Modulating the receptor specificity of the influenza viruses, to bind either α2,3-SA and α2,6-SA receptors, can confer an optimal competitive advantage on a viral strain *in vivo*. For example, the T187P + M227L double mutation in the H9N2 virus HA protein improves its affinity for its receptor and greatly improves viral attachment to mouse lung tissue, thereby increasing the proliferation and pathogenicity of the virus in mice [25,26]. Humans have receptor structures that strongly express α2,6-SA in the upper airways, and a greater abundance of α2,3-SA on bronchial epithelial cells and type II alveolar cells in the lower respiratory tract [27–29]. The H9N2 virus Q226L variant increased the virus's binding affinity for the α2,6-SA receptor and the airborne transmission ability of the virus in ferrets [19]. Pigs predominantly express both receptors (α2,3-SA and α2,6-SA) and were more susceptible to the Q226 variant (55%, 25/45) than to the L226 variant (42%, 19/45) [30]. A previous report indicated that the HA L226Q mutation caused a complete shift from α2,6-SA to α2,3-SA receptor in the poultry H9N2 virus receptor binding preference [31]. In this study, our results showed that L226Q enhanced the binding of H9N2 to the α2,3-SA receptor while reducing its binding to the α2,6-SA receptor, generating a dual receptor-binding phenotype. The L226Q mutation enhances the binding affinity

of H9N2 for mouse lung tissue, increases the virus's replication in the mouse respiratory tract, induces a stronger inflammatory response in the mouse lung, and enhances the pathogenicity of H9N2 in mice. Both RG HB-1631 and RG HB-1631-226Q viruses were detected in small amounts in the small intestines (Fig. S6) of the infected mice but did not display more extensive tissue tropism. Although the H9N2 viruses that infect humans commonly contain HA 226L [32], viruses with the HA L226Q mutation replicated more efficiently in the human lower respiratory tract where α2,3-SA is the main receptor [33], posing a threat to human health.

In summary, we have identified a wt H9N2 virus from human cases with a HA L226Q mutation. We have demonstrated that this mutation arises in a proportion of viruses during replication in a mouse model, alters the viral phenotype, and induces lethal infections in mice. These findings provide valuable insight into the mechanisms underlying the pathogenicity of H9N2 virus in humans, potentially informing the development of effective prevention and control strategies.

Funding

This work was supported by the National Key Research and Development Program of China (grant number 2021YFC2300100); the National Nature Science Foundation of China (grant number 81971941).

Author contributions

Min Tan: Conceptualization, Data curation, Writing – original draft. **Ye Zhang**: Resources, Methodology. **Hong Bo**: Investigation, Supervision. **Xiyan Li**: Validation, Methodology. **Shumei Zou**: Investigation. **Lei Yang**: Methodology, Project administration. **Jia Liu**: Formal analysis. **Qi Chen**: Data curation. **Xiaohao Xu**: Data curation. **Wenfei Zhu**: Funding acquisition, Project administration. **Dayan Wang**: Formal analysis, Conceptualization.

Acknowledgments

We sincerely thank the authors and laboratories who shared the H9 AIV sequences in GISAID and the GenBank database. This article is solely the responsibility of the authors and does not represent the views of China CDC or other organizations.

Declaration of competing interest

The authors declare that they have no known competing financial interests or personal relationships that could have appeared to influence the work reported in this paper.

Data available statement

The data that support the findings of this study are available on request from the corresponding.

Ethics statement

Not applicable.

Informed consent

Not applicable.

Supplementary materials

Supplementary material associated with this article can be found, in the online version, at doi:10.1016/j.imj.2024.100090.

References

[1] A. Fusaro, I. Monne, A. Salviato, et al., Phylogeography and evolutionary history of reassortant H9N2 viruses with potential human health implications, J Virol 85 (16) (2011) 8413–8421, doi:10.1128/JVI.00219-11.
[2] Y. Bi, J. Li, S. Li, et al., Dominant subtype switch in avian influenza viruses during 2016-2019 in China, Nat Commun 11 (1) (2020) 5909, doi:10.1038/s41467-020-19671-3.
[3] T.H.P. Peacock, J. James, J.E. Sealy, et al., A global perspective on H9N2 avian influenza virus, Viruses 11 (7) (2019) E620, doi:10.3390/v11070620.
[4] P.J. Homme, B.C. Easterday, "Avian influenza virus infections. I. Characteristics of influenza A-turkey-Wisconsin-1966 virus," (in eng), Avian Dis 14 (1) (1970) 66–74.
[5] C. Li, S. Wang, G. Bing, et al., Genetic evolution of influenza H9N2 viruses isolated from various hosts in China from 1994 to 2013, Emerg Microbes Infect 6 (11) (2017) e106, doi:10.1038/emi.2017.94.
[6] J. Wang, X. Jin, J. Hu, et al., Genetic evolution characteristics of genotype G57 virus, A dominant genotype of H9N2 avian influenza virus, Front. Microbiol. 12 (2021) 633835, doi:10.3389/fmicb.2021.633835.
[7] W. Qi, X. Zhou, W. Shi, et al., Genesis of the novel human-infecting influenza a(H10N8) virus and potential genetic diversity of the virus in poultry, China, Euro Surveill 19 (25) (2014) 20841, doi:10.2807/1560-7917.es2014.19.25.20841.
[8] A.N. Cauthen, D.E. Swayne, S. Schultz-Cherry, et al., Continued circulation in China of highly pathogenic avian influenza viruses encoding the hemagglutinin gene associated with the 1997 H5N1 outbreak in poultry and humans, J Virol 74 (14) (2000) 6592–6599, doi:10.1128/jvi.74.14.6592-6599.2000.
[9] Y. Chen, T. Bai, Y. Shu, Poultry to human passport: cross-species transmission of zoonotic H7N9 avian influenza virus to humans, Zoonoses 2 (2022) 4, doi:10.15212/ZOONOSES-2021-0026.
[10] M. Hu, Y. Jin, J. Zhou, et al., Genetic characteristic and global transmission of influenza A H9N2 virus, Front. Microbiol. 8 (2017) 2611, doi:10.3389/fmicb.2017.02611.
[11] X. Dong, L. Soong, Emerging and re-emerging Zoonoses are major and global challenges for public health, Zoonoses 1 (2021) 2737–7466, doi:10.15212/ZOONOSES-2021-00012021.
[12] WHO. Avian Influenza Weekly Update Number 830. Available at: https://www.who.int/. (Accessed October 20, 2023).
[13] R.K. Ravi, K. Walton, M. Khosroheidari, MiSeq: a next generation sequencing platform for genomic analysis, Methods Mol Biol 1706 (2018) 223–232, doi:10.1007/978-1-4939-7471-9_12.
[14] D.R. Zerbino, E. Birney, Velvet: algorithms for *de novo* short read assembly using de Bruijn graphs, Genome Res 18 (5) (2008) 821–829, doi:10.1101/gr.074492.107.
[15] B. Langmead, S.L. Salzberg, Fast gapped-read alignment with bowtie 2, Nat Meth 9 (4) (2012) 357–359, doi:10.1038/nmeth.1923.
[16] P.M. Kendal AP, J.J. Skehel, Concepts and procedures for laboratory-based influenza surveillance, World Health Organization, Geneva, 1982.
[17] Y.Y. Zhang, Y.F. Huang, J. Liang, et al., Improved up-and-down procedure for acute toxicity measurement with reliable LD(50) verified by typical toxic alkaloids and modified Karber method, BMC Pharmacol Toxicol 23 (1) (2022) 3, doi:10.1186/s40360-021-00541-7.
[18] H. Jung, S.C. Choi, Sequential method of estimating the LD50 using a modified up-and-down rule, J Biopharm Stat 4 (1) (1994) 19–30, doi:10.1080/10543409408835069.
[19] H. Wan, E.M. Sorrell, H. Song, et al., Replication and transmission of H9N2 influenza viruses in ferrets: evaluation of pandemic potential, PLoS One 3 (8) (2008) e2923, doi:10.1371/journal.pone.0002923.

[20] J. Wei, L. Zheng, X. Lv, et al., Analysis of influenza virus receptor specificity using glycan-functionalized gold nanoparticles, ACS Nano 8 (5) (2014) 4600–4607, doi:10.1021/nn5002485.
[21] Y. Zhao, Z. Yu, L. Liu, et al., Adaptive amino acid substitutions enhance the virulence of a novel human H7N9 influenza virus in mice, Vet Microbiol 187 (2016) 8–14, doi:10.1016/j.vetmic.2016.02.027.
[22] X. Sang, A. Wang, T. Chai, et al., Rapid emergence of a PB2-E627K substitution confers a virulent phenotype to an H9N2 avian influenza virus during adaption in mice, Arch Virol 160 (5) (2015) 1267–1277, doi:10.1007/s00705-015-2383-5.
[23] F. Yang, X. Zhang, F. Liu, et al., Rapid emergence of a PB2 D701N substitution during adaptation of an H9N2 avian influenza virus in mice, Arch Virol 167 (11) (2022) 2299–2303, doi:10.1007/s00705-022-05536-1.
[24] J. Wang, Y. Sun, Q. Xu, et al., Mouse-adapted H9N2 influenza A virus PB2 protein M147L and E627K mutations are critical for high virulence, PLoS One 7 (7) (2012) e40752, doi:10.1371/journal.pone.0040752.
[25] K. Liu, Y. Guo, H. Zheng, et al., Enhanced pathogenicity and transmissibility of H9N2 avian influenza virus in mammals by hemagglutinin mutations combined with PB2-627K, Virol Sin 38 (1) (2023) 47–55, doi:10.1016/j.virs.2022.09.006.
[26] K. Liu, X. Wang, D. Jiang, et al., Pathogenicity and transmissibility of an H9N2 avian influenza virus that naturally harbors the mammalian-adaptive molecular factors in the hemagglutinin and PB2 proteins, J Infect 82 (2) (2021) e22–e23, doi:10.1016/j.jinf.2020.09.009.
[27] S.S. Lakdawala, A.R. Shih, A. Jayaraman, et al., Receptor specificity does not affect replication or virulence of the 2009 pandemic H1N1 influenza virus in mice and ferrets, Virology 446 (1–2) (2013) 349–356, doi:10.1016/j.virol.2013.08.011.
[28] A. Jayaraman, A. Chandrasekaran, K. Viswanathan, et al., Decoding the distribution of glycan receptors for human-adapted influenza A viruses in ferret respiratory tract, PLoS One 7 (2) (2012) e27517, doi:10.1371/journal.pone.0027517.
[29] X. Li, J. Shi, J. Guo, et al., Genetics, receptor binding property, and transmissibility in mammals of naturally isolated H9N2 Avian Influenza viruses, PLoS Pathog 10 (11) (2014) e1004508, doi:10.1371/journal.ppat.1004508.
[30] K. Shinya, M. Ebina, S. Yamada, et al., Avian flu: influenza virus receptors in the human airway, Nature 440 (7083) (2006) 435–436, doi:10.1038/440435a.
[31] A.O. Obadan, J. Santos, L. Ferreri, et al., Flexibility *in vitro* of amino acid 226 in the receptor-binding site of an H9 subtype influenza A virus and its effect *in vivo* on virus replication, tropism, and transmission, J. Virol. 93 (6) (2019) e02011–e02018, doi:10.1128/JVI.02011-18.
[32] T.P. Peacock, J.E. Sealy, W.T. Harvey, et al., Genetic determinants of receptor-binding preference and zoonotic potential of H9N2 avian influenza viruses, J Virol 95 (5) (2021) e01651–20, doi:10.1128/JVI.01651-20.
[33] A. Gambotto, S.M. Barratt-Boyes, M.D. de Jong, et al., Human infection with highly pathogenic H5N1 influenza virus, Lancet 371 (9622) (2008) 1464–1475, doi:10.1016/S0140-6736(08)60627-3.